International Journal of Heat and Mass Transfer 51 (2008) 6254–6258

Contents lists available at ScienceDirect

International Journal of Heat and Mass Transfer

journal homepage: www.elsevier.com/locate/ijhmt

New analytical model for heat transfer efficiency of metallic honeycomb structures

Shutian Liu *, Yongcun Zhang, Peng Liu

State Key Laboratory of Structural Analysis for Industrial Equipment, Department of Engineering Mechanics, Dalian University of Technology, Dalian 116024, PR China

ARTICLE INFO

Article history:
Received 11 February 2007
Received in revised form 29 April 2007
Available online 23 July 2008

Keywords:
Active cooling
Sandwich panels
Prismatic cores
Metallic honeycombs
Transfer matrix method

ABSTRACT

In this paper, a new analytical model is presented to investigate the heat transfer performance of sandwich metallic honeycomb structures under the forced convection conditions. The new method overcomes the approximations in the corrugated wall model (also called the modified fin analogy model), the heat transfer efficiency predicted by this new method is consistently lower than that predicted by the corrugated wall model and is higher than that by the effective medium model. Compared with the corrugated wall model and the effective medium model, the new method gives the results closer to the numerical simulation results, which indicates that the method is accurate.

1. Introduction

Honeycombs, 2-D prismatic cellular metals, have emerged as promising multifunctional material systems [1–3]. They have a combination of properties that can be tailored to make them suitable for a range of applications such as structural load support, thermal management, impact energy absorption, sound absorption, fuel cell, energy storage, and others. The properties that appear most attractive are those that govern their use as cores for panels or shells having lower weight than competing materials.

Prismatic structures have one easy flow direction and have attracted significant interest for heat sink application including compact electronic cooling devices and ultra-light actively cooled aerospace structures. Numerous studies have been developed [4–14], thereinto, there are two analytical models used to describe the characteristic of heat transfer in two-dimensional prismatic structures with forced convection. One is the corrugated wall model [4,5] (also called the modified fin analogy model [6,7]). The other is the effective medium model [5]. The effective medium model uses volume averaging technique and somewhat underestimates the heat dissipation because of the assumption that the conduction of heat occurs predominantly normal to the convective flow. The corrugated wall approach can model the detailed cellular structure, thus it was often adopted in latter works. However, this method is also an approximate model.

There are two steps adopted to solve the thermal fields in the corrugated wall model. Firstly, the analysis of heat transfer is performed for the corrugated walls by excluding the effects of fins. Then, the contribution from the fin is added according to the energy balance. Lu said in his paper [4]: except for the effects of fin attachments which are modeled approximately, the approach is felt to be fairly accurate. However, an important aspect is neglected. The contribution of heat loss from fin attachment is about one third of the total heat loss for regular hexagonal honeycomb structures and about the half of the total heat loss for regular rectangular honeycomb structures, but the temperature field of a single corrugated wall is solved by excluding the effects of fins and then is used to decide the heat loss of the corrugated wall. Obviously, the temperature field obtained is not accurate, so that the heat loss of the corrugated wall is also approximate.

In this paper, the transfer matrix method is presented as a new analytical model to analyze the heat transfer for the corrugated walls and fins simultaneously. So it can avoid the approximations in the corrugated model. The article is organized as follows. The model is described in Section 2. Section 3 presents the mathematical formulation of transfer matrix method. The comparisons with other analytical models and the numerical simulation results are discussed and show the validity of method in Section 4 and summary follow.

2. The model

The prototypical compact heat transfer exchanger design is shown in Fig. 1. The cooling fluid, with velocity v_0, temperature T_0, pressure p_0, is forced to flow across a two-dimensional metal array of thickness H sandwiched between two flat rectangular plates of length L and width W. The plates are assumed to be thin and have large thermal conductivity so that the temperature is assumed to be constant along thickness direction. It is insulated on

* Corresponding author. Tel./fax: +86 411 84706149.
E-mail address: stliu@dlut.edu.cn (S. Liu).

0017-9310/$ - see front matter © 2008 Elsevier Ltd. All rights reserved.
doi:10.1016/j.ijheatmasstransfer.2007.07.055

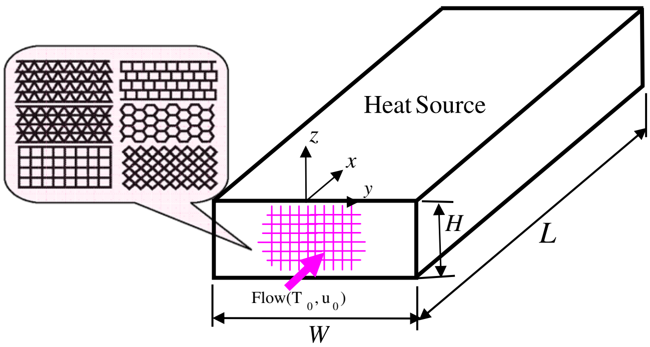

Fig. 1. Prototypical design of compact heat sink with two dimensional metal honeycombs for cooling by forced convection.

the left and right sides and is subjected to the heat sources on the bottom and top surface. The width of channel, W, is assumed to be much larger than the cellular size so that the thermal and hydraulic fields are independent of the coordinate y. Let ρ_f, v_f, μ_f and c_p denote the fluid density, kinematic viscosity, shear viscosity and specific heat constant pressure, respectively. In addition, the usual assumptions of the steady state laminar flow, and constant thermal/physical properties of both fluid and solid are made.

3. Transfer matrix method

Actually, any prismatic structures can be considered here. For the purpose of illustration, the regular hexagonal honeycomb structure (shown in Fig. 2a) is taken as a sample to describe the basic idea of transfer matrix method. Firstly, the heat sink is divided into periodic slices of equal width, as shown in Fig. 2b. Then, one analytical cell is selected along the corrugated wall direction, as shown in Fig. 2c. The variation of temperature T along the cell wall is governed by

$$\frac{\mathrm{d}^2T(x,\xi)}{\mathrm{d}\xi^2}-\frac{2h}{k_st}(T(x,\xi)-T_f(x))=0, \tag{1}$$

where $T_f(x)$ is the mean fluid temperature at the location with coordinate x and ξ is the local coordinate along the wall. k_s is the thermal conductivity ratio of solid wall and t the thickness of the cell wall. h is the local heat transfer coefficient and can be denoted by following expression for regular hexagonal structures

$$h=\frac{Nuk_f}{\sqrt{3}l\sqrt{1-\rho}}, \tag{2}$$

where Nu is Nusselt number, k_f is the thermal conductivity of cooling fluid, ρ is the relative density and l is the cell size.

Assuming

$$\widehat{T}(x,\xi)=T(x,\xi)-T_f(x), \tag{3}$$

$$\lambda^2=\frac{2h}{k_st}. \tag{4}$$

Eq. (1) can be rewritten as

$$\frac{\mathrm{d}^2\,\widehat{T}(x,\xi)}{\mathrm{d}\xi^2}-\lambda^2\,\widehat{T}(x,\xi)=0. \tag{1.1}$$

Subjected the boundary conditions that $\widehat{T}(x,\xi)=\widehat{T}_i$ at $\xi=0$ and $\widehat{T}(x,\xi)=\widehat{T}_j$ at $\xi=l$, the solution of Eq. (1.1) can be expressed as

$$\widehat{T}(x,\xi)=\frac{\sinh[\lambda(l-\xi)]}{\sinh(\lambda l)}\widehat{T}_i+\frac{\sinh(\lambda\xi)}{\sinh(\lambda l)}\widehat{T}_j. \tag{5}$$

Thus, the heat flux along the wall is

$$\begin{aligned}q(x,\xi)&=-k_st\frac{\mathrm{d}T(x,\xi)}{\mathrm{d}\xi}\\&=\lambda k_st\left(\frac{\cosh(\lambda(l-\xi))}{\sinh(\lambda l)}\widehat{T}_i(x)-\frac{\cosh(\lambda\xi)}{\sinh(\lambda l)}\widehat{T}_j(x)\right).\end{aligned} \tag{6}$$

The heat dissipation to the fluid through the corrugated wall of length l is

$$q_c=q(x,0)-q(x,l)=\lambda k_st\cdot\tanh(\lambda l/2)(\widehat{T}_i+\widehat{T}_j). \tag{7}$$

The temperature $\hat{T}_{j'}$ at the node j' should be the same with the temperature $\hat{T}_j$ at the node j according to the symmetry, so the heat loss to flow through the fin wall of length $l/2$ is

$$q_f=\frac{1}{2}\lambda k_st\cdot\tanh(\lambda l/2(\widehat{T}_j+\widehat{T}_{j'})=\lambda k_st\cdot\tanh(\lambda l/2)\widehat{T}_j. \tag{8}$$

The energy equilibrium equation can be expressed as below

$$\text{At node}\quad i\ q_i=q(x,0)=\lambda k_st\left(\frac{\cosh(\lambda l)}{\sinh(\lambda l)}\widehat{T}_i-\frac{1}{\sinh(\lambda l)}\widehat{T}_j\right), \tag{9}$$

$$\text{At node}\quad j\quad q_i-q_c-q_f=q_j. \tag{10}$$

Substituting the Eqs. (8) and (9) into the Eq. (10) yields

$$q_j=q_i-\lambda k_st\cdot\tanh(\lambda l/2)(\widehat{T}_i+2\widehat{T}_j). \tag{11}$$

From Eqs. (10) and (11), we can get the expression of q_j, $\widehat{T}_j$

$$q_j=[2\cosh(\lambda l)-1]q_i-\lambda k_st[2\sinh(\lambda l)-\tanh(\lambda l/2)]\widehat{T}_i \tag{12.1}$$

$$\widehat{T}_j=-\frac{\sinh(\lambda l)}{\lambda k_st}q_i+\cosh(\lambda l)\widehat{T}_i. \tag{12.2}$$

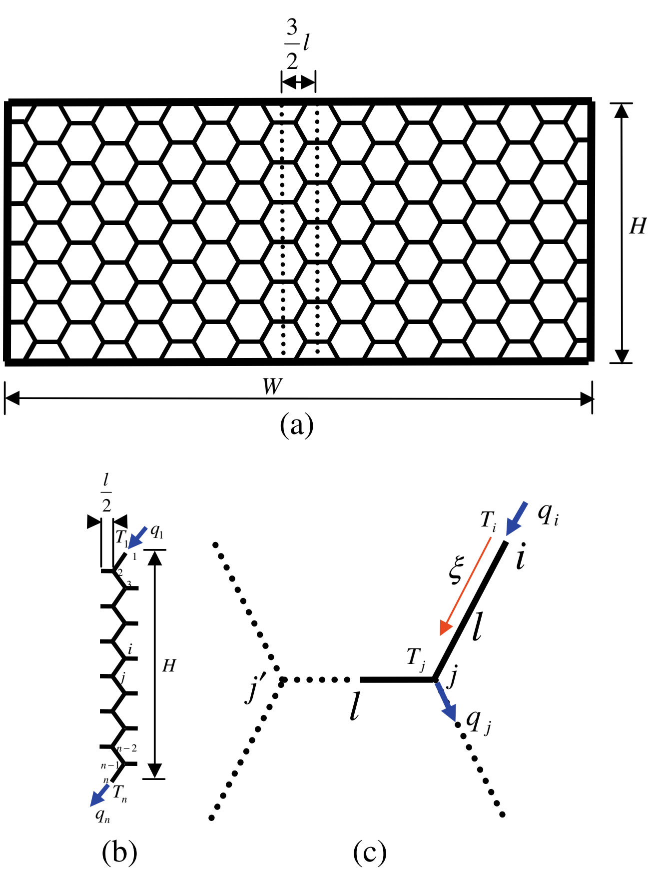

Fig. 2. (a) Cross-section of heat sink for regular hexagonal honeycombs, (b) corrugated wall with the fin attachments and (c) analytical cell (solid line).

Defining

$$\mathbf{\Gamma_i} = \begin{bmatrix} q_i \\ \widehat{T}_i \end{bmatrix}, \tag{13}$$

$$\mathbf{E} = \begin{bmatrix} 2\cosh(\lambda l) - 1 - \lambda k_s t[2\sinh(\lambda l) - \tanh(\lambda l/2)] \\ -\sinh(\lambda l)/(\lambda k_s t)\cosh(\lambda l) \end{bmatrix}, \tag{14}$$

Eqs. (12.1) and (12.2) can be written in matrix form as:

$$\mathbf{\Gamma}_j = \mathbf{E}\mathbf{\Gamma_i} \tag{15}$$

where the matrix **E** is defined as the transfer matrix.

The corrugated wall at the bottom shown in Fig. 2(b) has no fin attached. In this particular case, the transfer matrix can be expressed as

$$\mathbf{E}^* = \begin{bmatrix} \cosh(\lambda l) & -\lambda k_s t\sinh(\lambda l) \\ -\sinh(\lambda l)/(\lambda k_s t) & \cosh(\lambda l) \end{bmatrix} \tag{16}$$

which can be gained by a similar process expressed by Eqs. 10, 11, 13, 14 with $q_f = 0$ in Eq. (10).

From Eq. (15), we have following expressions for the structure shown in Fig. 2(b):

$$\mathbf{\Gamma}_2 = \mathbf{E}\mathbf{\Gamma}_1,$$
$$\mathbf{\Gamma}_3 = \mathbf{E}\mathbf{\Gamma}_2 = \mathbf{E}^2\mathbf{\Gamma}_1$$
$$\mathbf{\Gamma}_4 = \mathbf{E}\mathbf{\Gamma}_3 = \mathbf{E}^3\mathbf{\Gamma}_1$$
$$\cdots\cdots$$
$$\mathbf{\Gamma}_{n-1} = \mathbf{E}\mathbf{\Gamma}_{n-2} = \mathbf{E}^{n-2}\mathbf{\Gamma}_1$$
$$\mathbf{\Gamma}_n = \mathbf{E}^*\mathbf{\Gamma}_{n-1} = \mathbf{E}^*\mathbf{E}^{n-2}\mathbf{\Gamma}_1$$

Define

$$\mathbf{K} = \mathbf{E}^*\mathbf{E}^{n-2} = \begin{bmatrix} k_{11} & k_{12} \\ k_{21} & k_{22} \end{bmatrix} \tag{17}$$

where

$$k_{11} = \varphi_{11}(\lambda, l), \quad k_{12} = -\lambda k_s t\varphi_{12}(\lambda, l),$$
$$k_{21} = -\varphi_{21}(\lambda, l)/(\lambda k_s t), \quad k_{22} = \varphi_{22}(\lambda, l) \tag{18}$$

then

$$\mathbf{\Gamma}_n = \mathbf{K}\mathbf{\Gamma}_1 \tag{19}$$

where $\mathbf{\Gamma}_1 = [q_1 \quad \widehat{T}_1]$, $\mathbf{\Gamma}_n = [q_n \quad \widehat{T}_n]$ and $\widehat{T}_1, \widehat{T}_n, q_1, q_n$ are the temperature and flux on the two boundaries, respectively. If we know the two of them, the other two can be gained easily.

There are usually two classic types of heat transfer boundary conditions considered: One applies when both plates are isothermal with uniform temperature T_w and the other holds if the plates release uniform heat flux (isoflux) q_0. According to the study of Lu [4], the resulting expression of the overall heat transfer coefficient $\bar{h}$ is identical for these two types of boundary conditions. The only difference is that the Nu is 3.35 for the isothermal surface and is 4.021 for the constant heat flux surface. Thus, only the isothermal surface is discussed in this paper.

Because the temperatures of both the upper and bottom surface plates are T_w, i.e., $\widehat{T}_1 = \widehat{T}_n = T_w - T_f(x)$, following relation can be obtained from Eq. (19)

$$\begin{Bmatrix} q_n \\ T_w - T_f(x) \end{Bmatrix} = \begin{bmatrix} k_{11} & k_{12} \\ k_{21} & k_{22} \end{bmatrix} \begin{Bmatrix} q_1 \\ T_w - T_f(x) \end{Bmatrix} \tag{20}$$

Thus, the heat flux can be expressed as

$$q_1 = \lambda k_s t\Phi(\lambda, l)(T_w - T_f(x)) \tag{21}$$

where

$$\Phi(\lambda, l) = \frac{\varphi_{22}(\lambda, l) - 1}{\varphi_{21}(\lambda, l)} \tag{22}$$

Owing to the symmetry, the heat flux to the cooling fluid from bottom surface is equal to that from upper surface. Thus, the total heat loss is

$$q(x) = 2q_1 = 2\lambda k_s t\Phi(\lambda, l)(T_w - T_f(x)) \tag{23}$$

The mean fluid temperature $T_f(x)$ is calculated by imposing energy conservation for the control volume of length $\mathrm{d}x$

$$\dot{m}c_p[T_f(x + \mathrm{d}x) - T_f(x)] = [N_s q(x) + q_w(x)]\mathrm{d}x \tag{24}$$

where $\dot{m} = \rho_f u_0 HW$ is the mass flow rate at the entrance to the heat sink, ρ_f, c_p are the density and capacity of the cooling fluid, respectively. N_s(=$c_n W/l$) is the total number of slices over width W, and

$$q_w(x) = 2h\left(W - \frac{\sqrt{3}}{2}N_s t\right)[T_w - T_f(x)] \tag{25}$$

is the heat flux into the fluid from both face sheets directly.

Combination Eqs. (23) and (24) gives rise to an ordinary differential equation for the mean fluid temperature $T_f(x)$. The solution is

$$T_w - T_f(x) = (T_w - T_0)\exp(-x/L^*) \tag{26}$$

where L^* is the characteristic length scale given by

$$L^* = \frac{\rho_f c_p u_0 H}{2h}\left[1 - \frac{1}{\sqrt{3}}\frac{t}{l} + \frac{2}{3}\sqrt{\frac{2\sqrt{3}k_s\sqrt{1-\rho}}{Nuk_f}\frac{t}{l}}\Phi(\lambda, l)\right]^{-1} \tag{27}$$

The overall heat transfer coefficient, $\bar{h}$ of the heat sink is defined as

$$\bar{h} = \frac{Q}{2LW\Delta T_m} \tag{28}$$

where ΔT_m is the logarithmic mean temperature difference denoted by

$$\Delta T_m = \frac{(T_w - T_0) - (T_w - T_e)}{\ln[(T_w - T_0)/(T_w - T_e)]} \tag{29}$$

and Q is the total heat dissipation from the sandwich structure

$$Q = \dot{m}c_p(T_f(L) - T_0) = \rho_f c_p u_0 HW(T_w - T_0)\{1 - \exp(-L/L^*)\} \tag{30}$$

It can be readily verified that $\Delta T_m = T_w - \bar{T}_f$. The resulting expression for $\bar{h}$ is

$$\bar{h} = \frac{Nuk_f}{\sqrt{3}l\sqrt{1-\rho}}\left[1 - \frac{1}{\sqrt{3}}\frac{t}{l} + \frac{2}{3}\sqrt{\frac{2\sqrt{3}k_s\sqrt{1-\rho}}{Nuk_f}\frac{t}{l}}\Phi(\lambda, l)\right] \tag{31}$$

Notice that $\bar{h}$ is independent of x and it is an intrinsic feature of heat transfer in ducts with uniform temperature walls.

4. Discussion

For convenience, the dimensionless indices developed by Lu [4] is utilized to evaluate the performance of metallic honeycomb structure

$$I = c_1\bar{h}/\Delta p \tag{32}$$

where

$$c_1 = v_f\rho_f u_0/k_s \tag{33}$$

$$\frac{\Delta p}{L} = \frac{c_f c_a^2}{8}\frac{\rho_f v_f u_0}{(1-\rho)^2 l^2} \tag{34}$$

and v_f is the kinematical viscosity, c_f the frictional coefficient, u_0 the velocity of fluid at the inlet, and c_a the shape factor and equal 2.31 for hexagonal cells.

For hexagonal honeycomb structures, the dimensionless index determined by the transfer matrix method can be expressed as

$$I = \frac{2Nuk_f(1-\rho)^{3/2}l}{k_s c_f c_a^L}\left[1 - \frac{1}{\sqrt{3}}\frac{t}{l} + \frac{2}{3}\sqrt{\frac{2\sqrt{3}k_s\sqrt{1-\rho}}{Nuk_f}\frac{t}{l}}\Phi(\lambda, l)\right] \quad (35)$$

In [5], this dimensionless index for corrugated wall model of hexagonal honeycomb structure is given by

$$I = \frac{2Nu \cdot k_f(1-\rho)^{3/2}l}{k_s c_f c_a^L} \times \left[1 - \frac{c_n c_w t}{l} + 2c_n n\sqrt{\frac{2k_s t\sqrt{1-\rho}}{c_a Nu \cdot k_f l}}\tanh\left(\frac{c_H H}{2l}\sqrt{\frac{c_a Nu \cdot k_f l}{2k_s t\sqrt{1-\rho}}}\right)\right] \quad (36)$$

where $c_n = 2/3$, $c_w = \sqrt{3}/2$, $n = 1$, $c_H = 2/\sqrt{3}$, the detailed definition of these parameters can be referred to [5]. For the effective medium model

$$I = \frac{4l(1-\rho)^2}{c_f c_a k_s L}\left\{\sqrt{Nuk_f c_{kz} k_s \rho}\tanh\left(\frac{c_a H}{4l}\sqrt{\frac{Nuk_f}{c_{kz}k_s\rho}}\right)\right\} \quad (37)$$

These three methods are all employed below to investigate the heat transfer efficiency. The parameters used are $l = 1$ mm, $H/l = 10\sqrt{3}$, $L/l = 50$, $k_s = 200$ W/mK, $k_f = 0.026$ W/mK for the regular hexagonal structure. The predicted heat transfer efficiency I againstρ from three models is shown in Fig. 3. Although these three models exhibit the same trend, the predicted index I from the transfer matrix method is consistently lower than that from the corrugated wall model and is higher than that from the effective medium model.

To verify the accuracy of the transfer matrix method, the head transfer efficiency of a hexagonal honeycomb structure is calculated by solving the fluid dynamic problem by use of the finite volume method. In this calculation, the specific boundary conditions are given as following: The temperature of both the upper and bottom plates is 100 °C and the fluid temperature is 10 °C at the inlet, the mass flow rate is 1.0×10^{-5} kg/s; A pressure-outlet boundary condition with zero gauge pressure is employed at the exit of the cell duct; Symmetrical boundary conditions for all side surfaces in the width-direction are employed. The inner surfaces of each cell are set as coupled thermal conditions. The heat capacity and viscosity of the cooling fluid are 1006.43 J/kg K and 1.7894×10^{-5} kg/m s. For simplify, one periodic structure in width direction shown in Fig. 4 is used. The results are also shown in Fig. 3. The data shows that the transfer matrix method is closer to the results of the finite volume method compared to the results of corrugated wall model and effective medium model, which indicates to some extent that the transfer matrix method is more precise compared to other two models considered in this paper.

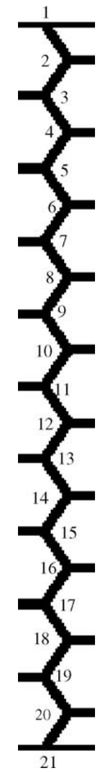

Fig. 4. Nodes at the inlet cross-section along the height direction.

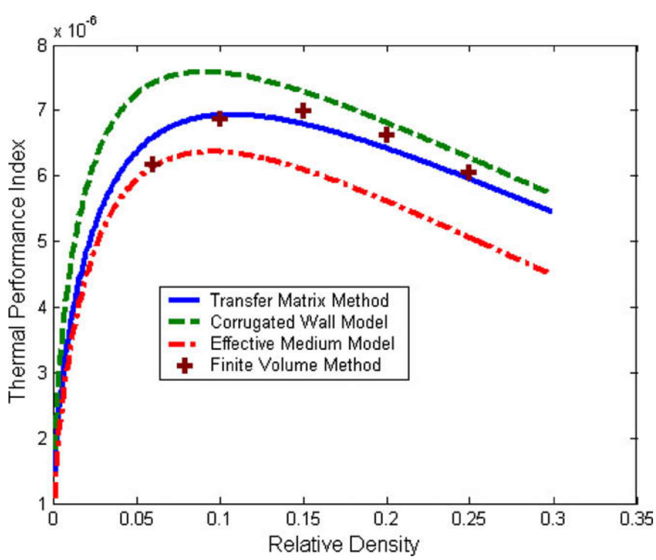

Fig. 3. Thermal performance index of sandwich structure with hexagonal honeycomb core plotted as a function of relative density. Parameters include $l = 1$ mm, $H/l = 10\sqrt{3}$, $L/l = 50$, $k_s = 200$ W/mK, $k_f = 0.026$ W/mK.

Table 1
Temperature of the nodes at the inlet section along the height direction shown in Fig. 4

Nodes	$\rho = 0.01$		$\rho = 0.2$	
	Corrugated wall model	Transfer matrix method	Corrugated wall model	Transfer matrix method
1	100.0000	100.0000	100.0000	100.0000
2	81.0530	77.1424	97.6219	96.5925
3	66.2635	60.1771	95.5314	93.5847
4	54.7659	47.6169	93.6679	90.9625
5	45.8877	38.3576	92.0799	88.7139
6	39.1093	31.5872	90.7443	86.8285
7	34.0341	26.7114	89.6571	85.2977
8	30.3652	23.3024	88.8149	84.1143
9	27.8878	21.0608	88.2153	83.2729
10	26.4571	19.7900	87.8562	82.7696
11	25.9893	13.3785	87.7366	82.6021
12	26.4571	19.7900	87.8562	82.7696
13	27.8878	21.0608	87.2153	83.2729
14	30.3652	23.3024	88.8149	84.1143
15	34.0341	26.7114	89.6571	85.2977
16	39.1093	31.5872	90.7443	86.8285
17	45.8877	38.3576	92.0799	88.7139
18	54.7659	47.6169	93.6679	90.9625
19	66.2635	60.1771	95.5314	93.5847
20	81.0530	77.1424	97.6219	96.5925
21	100.0000	100.0000	100.0000	100.0000

As discussed before, the first step in the corrugated wall model estimates the temperature field inaccurately and then such a trend is reinforced by the contribution from the fins added in the second step. In order to illustrate the temperature field, a specific numerical example is given. The temperature of both plates is 100 °C and the fluid temperature is 10 °C at the inlet, the temperature of every node at the inlet section along the height direction shown in Fig. 4 are listed in the Table 1 with different relative density 0.01 and 0.2. The data show that the temperature field of a single corrugated wall predicted from the corrugated wall model is higher than the transfer matrix method. An overestimated temperature field leads to the heat transfer efficiency I higher then the real case.

Because of ignoring the extra heat dissipation from the plate surface and fin attachments, the effective medium model underestimates the heat transfer efficiency I. Thus the real heat transfer efficiency lists between the corrugated wall model and the effective medium model. By analyzing the heat transfer both in the corrugated walls and fins simultaneously, the transfer matrix method can avoid the deficiency of the corrugated wall model and still can model the detailed structure. Thus, the transfer matrix method is more accurate method for predicting the heat transfer efficiency of honeycomb structures.

5. Summary

The transfer matrix method as a new analytical method is presented to investigate the heat transfer performance of sandwiched metallic honeycomb structures under the forced convection conditions. Similar with the corrugated wall model, the transfer matrix method can model the detailed cellular structure, but it avoids the approximation in the corrugated model. Comparison of the transfer matrix method with the corrugated wall mode and effective medium model shows that these three methods are all able to predict the heat transfer efficiency accurately, and the heat transfer efficiency predicted by the transfer matrix method is more precise.

Acknowledgements

This research is supported in part by the NSFC through the Grant Nos. (10332010, 90205029, and 10421202), the national key basic research program of china through Grant No. 2006CB601205 and by the program for new century excellent talents in university of china (2004). The financial supports are gratefully acknowledged.

References

[1] Haydn N.G. Wadley, Multifunctional periodic cellular metals, Philos. Trans. Royal Soc. A 364 (2006) 31–68.
[2] Lorna J. Gibson, Michael F. Ashby, Cellular Solids: Structure and Properties, second ed., Cambridge University Press, 1997.
[3] A. G Evans, J.W. Hutchinson, N.A. Fleck, M. F Ashby, H.N.G. Wadley, The topological design of multifunctional cellular metals, Progress Mater. Sci. 46 (2001) 309–327.
[4] T.J. Lu, Heat transfer efficiency of metal honeycomb, Int. J. Heat Mass Transfer 42 (1999) 2031–2040.
[5] S. Gu, T.J. Lu, A.G. Evans, On the design of two-dimensional cellular metals for combined heat dissipation and structural load capacity, Int. J. Heat Mass Transfer 44 (2001) 2163–2175.
[6] T.J. Lu, L. Valdevit, A.G. Evans, Active cooling by metallic sandwich structures with periodic cores, Prog. Mater. Sci. 50 (2005) 789–815.
[7] L. Valdevit, A. Pantano, H.A. Stone, A.G. Evans, Optimal active cooling performance of metallic sandwich panels with prismatic cores, Int. J. Heat Mass Transfer 49 (2006) 3819–3830.
[8] T. Wen, J. Tian, T.J. Lu, D.T. Queheillalt, H.N.G. Wadley, Forced convection in metallic honeycombs structures, Int. J. Heat Mass Transfer 49 (2006) 3313–3324.
[9] C.C. Seepersad, B.M. Dempsey, J.K. Allen, F. Mistree, D.L. McDowell, Design of multifunctional honeycomb materials, AIAA J. 42 (2004) 1025–1033.
[10] R.S. Kumar, D.L. McDowell, Rapid preliminary design of rectangular linear cellular alloys for maximum heat transfer, AIAA J. 42 (2004) 1652–1661.
[11] Bo Wang, G. D. Cheng, Bin Wang, Multifunctional optimum design of honeycomb structures. In: The proceedings of The Fourth China-Japan-Korea Joint Symposium on Optimization of Structural and Mechanical Systems Kunming, China, November, 6–9, 2006, pp. 267–272.
[12] Bo. Wang, G.D. Cheng, Bin Wang, Multifunctional optimum design of honeycomb structures, The Proceedings of The Fourth China–Japan–Korea Joint Symposium on Optimization of Structural and Mechanical Systems Kunming, 6–9 (2006) 267–272.
[13] B.M. Dempsey, S. Eisele, D.L. McDowell, Heat sink application of extruded metal honeycomb materials, Int. J. Heat Mass Transfer 48 (2005) 527–535.
[14] A.M. Hayes, A. Wang, B.M. Dempsey, D.L. McDowell, Mechanics of linear cellular alloys, Mech. Mater. 36 (2004) 691–713.